

TRACE/PARCS ANALYSIS OF ATWS WITH INSTABILITY FOR A MELLLA+ BWR/5

L. Cheng, J. Baek, A. Cuadra, A. Aronson, and D. Diamond

Brookhaven National Laboratory Nuclear Science and Technology Department
Brookhaven National Laboratory, P.O. Box 5000, Upton, NY 11973-5000
cheng@bnl.gov

P. Yarsky

Nuclear Regulatory Commission Office of Nuclear Regulatory Research
U.S. Nuclear Regulatory Commission, MS CSB-3A07M, Washington, DC 20555-0001
peter.yarsky@nrc.gov

ABSTRACT

A TRACE/PARCS [1, 2] model has been developed to analyze anticipated transient without SCRAM (ATWS) events for a boiling water reactor (BWR) operating in the maximum extended load line limit analysis-plus (MELLLA+) expanded operating domain. The MELLLA+ domain expands allowable operation in the power/flow map of a BWR to low flow rates at high power conditions [3]. Such operation exacerbates the likelihood of large amplitude power/flow oscillations during certain ATWS scenarios [4]. The regulatory purpose of the current work is to demonstrate the application of TRACE/PARCS to analyze ATWS events for MELLLA+ BWR plants resulting in large amplitude, unstable power/flow oscillations.

The TRACE/PARCS model simulates a BWR/5 plant operating at 120 percent of the originally licensed thermal power with a MELLLA+ flow control window extending down to 85 percent of the rated core flow rate.

Results from three representative cases (based on time in fuel cycle) are presented. The analysis shows that large amplitude power/flow oscillations, both core-wide and out-of-phase, arise following the establishment of natural circulation flow in the reactor pressure vessel (RPV) after the trip of the recirculation pumps and an increase in core inlet subcooling. The analysis also indicates a mechanism by which the fuel may experience heat-up that could result in localized fuel damage. TRACE predicts the heat-up to occur when the cladding surface temperature exceeds the minimum stable film boiling temperature after periodic cycles of dryout and rewet; and the fuel becomes “locked” into a film boiling regime. Further, the analysis demonstrates the effectiveness of the simulated manual operator actions to suppress the instability.

KEYWORDS

ATWS BWR MELLLA+ PARCS TRACE Instability

1. INTRODUCTION

The regulatory purpose of the current work is to demonstrate the application of TRACE/PARCS to analyze ATWS events for MELLLA+ BWR plants resulting in large amplitude, unstable power/flow oscillations. Operation in the MELLLA+ domain exacerbates the consequences of ATWS events owing

to the evolution of a higher power/flow ratio state following the trip of the recirculation pumps. Figure 1 illustrates a typical plant trajectory following a dual recirculation pump trip (2RPT) for a plant operating at originally licensed thermal power (OLTP) conditions and MELLLA+ conditions [3, 4]. The higher power/flow ratio conditions can result in highly unstable conditions, leading to large amplitude power/flow oscillations.

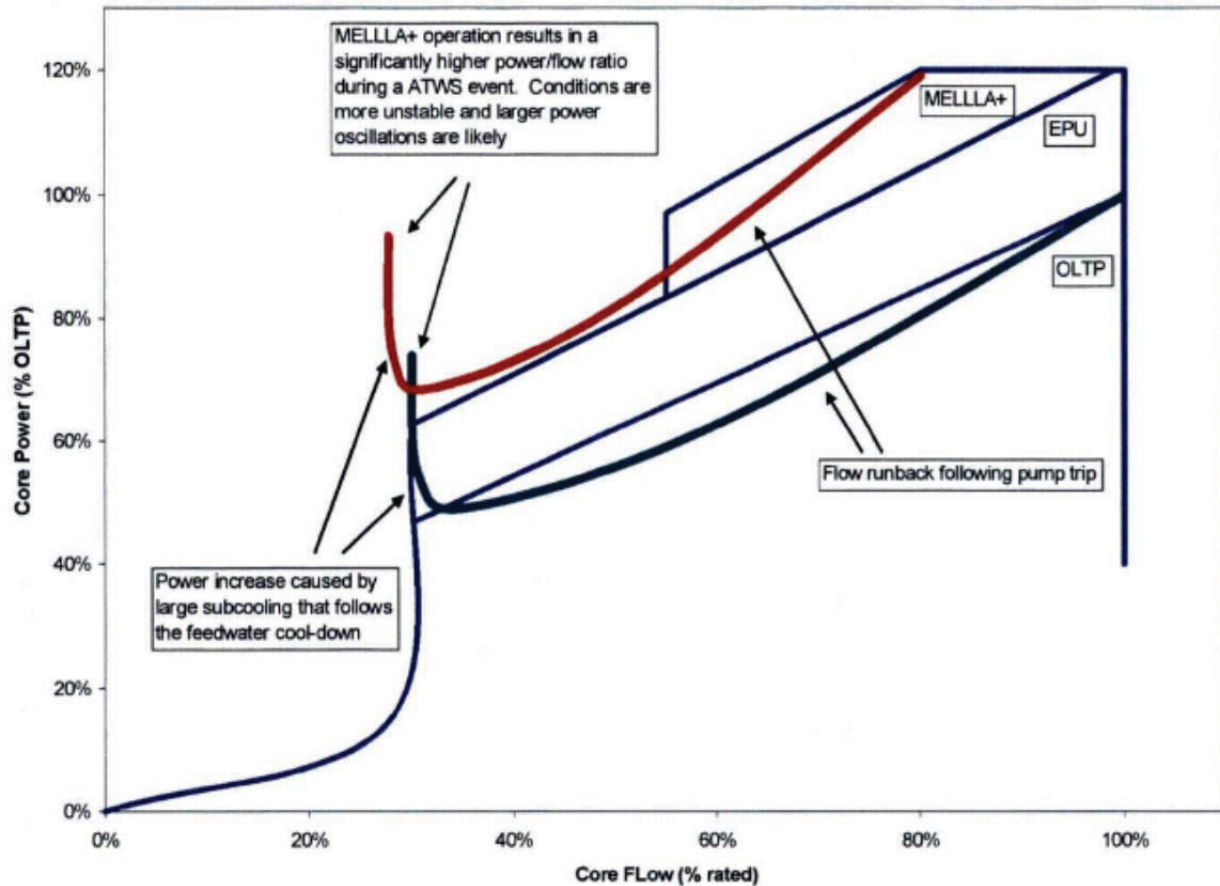


Figure 1. Evolution of Power and Flow Conditions during ATWS Following 2RPT [3, 4].

The Nuclear Regulatory Commission (NRC) systems analysis codes, TRACE [1] and PARCS [2], have been evaluated for applicability to analyze ATWS with instability (ATWS-I) for MELLLA+ BWRs [4]. The current work demonstrates the application by performing simulation of ATWS-I scenarios for a BWR/5 plant.

2. MODELING AND METHODOLOGY

The model is divided into two parts, the first being the TRACE systems model. This part of the overall model simulates the thermal-hydraulic and thermo-mechanical response of the plant and core. The second part of the model is the PARCS neutronic model. The PARCS part simulates the kinetic behavior of the core in response to changing conditions of the coolant and fuel. The two models are connected through a mapping interface that associates thermal-hydraulic channels with neutronic nodes. Detailed

discussions about developing the TRACE and PARCS models are presented in [5, 6]. The calculations were performed using a four-step methodology as described in [7].

2.1. TRACE System Model

The TRACE model of the BWR/5 plant consists of a number of hydraulic components and heat structures [5]. Fuel assemblies are modeled with CHAN components. A POWER component identifies CHANs for coupling with PARCS. Figure 2 is a node diagram providing the component view of the complete model. The model consists of a BWR vessel (with internals consisting of one jet pump, two control rod guidetubes, and two steam separators), one recirculation loop (representing the two recirculation loops) with recirculation pump and flow control valve, a feedwater line, a reactor core isolation cooling system (RCIC) line with option to draw from the condensate storage tank or the suppression pool, two standby liquid control system (SLCS) lines (for lower plenum and upper plenum injection), a main steamline with in-board and out-board main steam isolation valves and a branch to safety/relief/automatic depressurization system valves (SRVs and ADS), turbine control valve (TCV), and a primary containment (drywell and wetwell) with suppression pool cooler and passive heat structures (structural components). Control systems consisting of signal variables, control blocks and trips complete the TRACE model.

A three-element feedwater (FW) controller is included in the TRACE model to maintain reactor water level (RWL) at the desired level setpoint based on the following controller inputs: FW flow, steam flow, and RWL. Adjusting the RWL input to the controller allows simulation of operator actions to control RWL according to different emergency operating procedure strategies. The adjustment is in the form of a bias which represents the difference between the nominal level setpoint and the target water level. The controller input is the sum of the actual RWL and the bias. In the current work, a time based trip is used to modify the controller input bias to simulate operator actions to control RWL to the top of active fuel (TAF).

The function of the turbine bypass system (TBS) is simulated using the turbine control valve (TCV). The end of the steamline includes a TCV component attached to a BREAK component. The BREAK component is set to a fixed pressure that corresponds to the TBS desired pressure set point. In the steady-state calculation, the TCV position is determined to match a desired dome pressure. To simulate the TBS function during the transient, the TCV is opened, which applies the BREAK pressure boundary condition to the steamline that corresponds to the TBS setpoint.

The reactor is represented by a three dimensional VESSEL component with three radial rings, 17 axial levels, and one azimuthal sector. The core and the steam separators are in Rings 1 and 2 while the downcomer is in the 3rd (outer-most) Ring.

There are 764 fuel assemblies in the core and they are associated with the two inner radial rings in the VESSEL component, 616 assemblies in Ring 1 and 148 assemblies in Ring 2. Ninety-two of the fuel assemblies in Ring 2 are identified as peripheral assemblies because they are located on the outer edge of the core next to the core shroud. Each fuel assembly has 92 fuel rods and two water rods arranged in a 10x10 array with each water rod occupying four grid positions. There are three types of fuel rods: full length, partial length and gadolinia bearing fuel rods. They are grouped together as separate rod groups in the CHAN component. A fourth and fifth rod group represent the hot rod in an assembly and the water rods respectively.

The CHAN model incorporates three TRACE options: dynamic gas-gap in the fuel rod, modified Nuclear Fuel Industries correlation for fuel thermal conductivity and metal-water reaction [1]. These optional models use burnup information together with the gadolinia content in a fuel rod. The gap gas composition and initial oxide thickness on the clad are determined from FRAPCON results [6].

For ATWS-I, the complex neutronic-thermal-hydraulic coupling during periods of instability needs to be captured. In independent PARCS standalone steady-state calculations (with fixed thermal-hydraulic conditions), it was shown that for all points in the cycle the first harmonic had an axis of symmetry along the y-axis. Hence, 382 thermal-hydraulic channels (CHAN components) are modeled to represent all assemblies, taking into account half-core symmetry while allowing for first harmonic modes of oscillation. This approach allows the development of bi-modal oscillations, but does not allow the development of oscillations with a rotating symmetry plane [8].

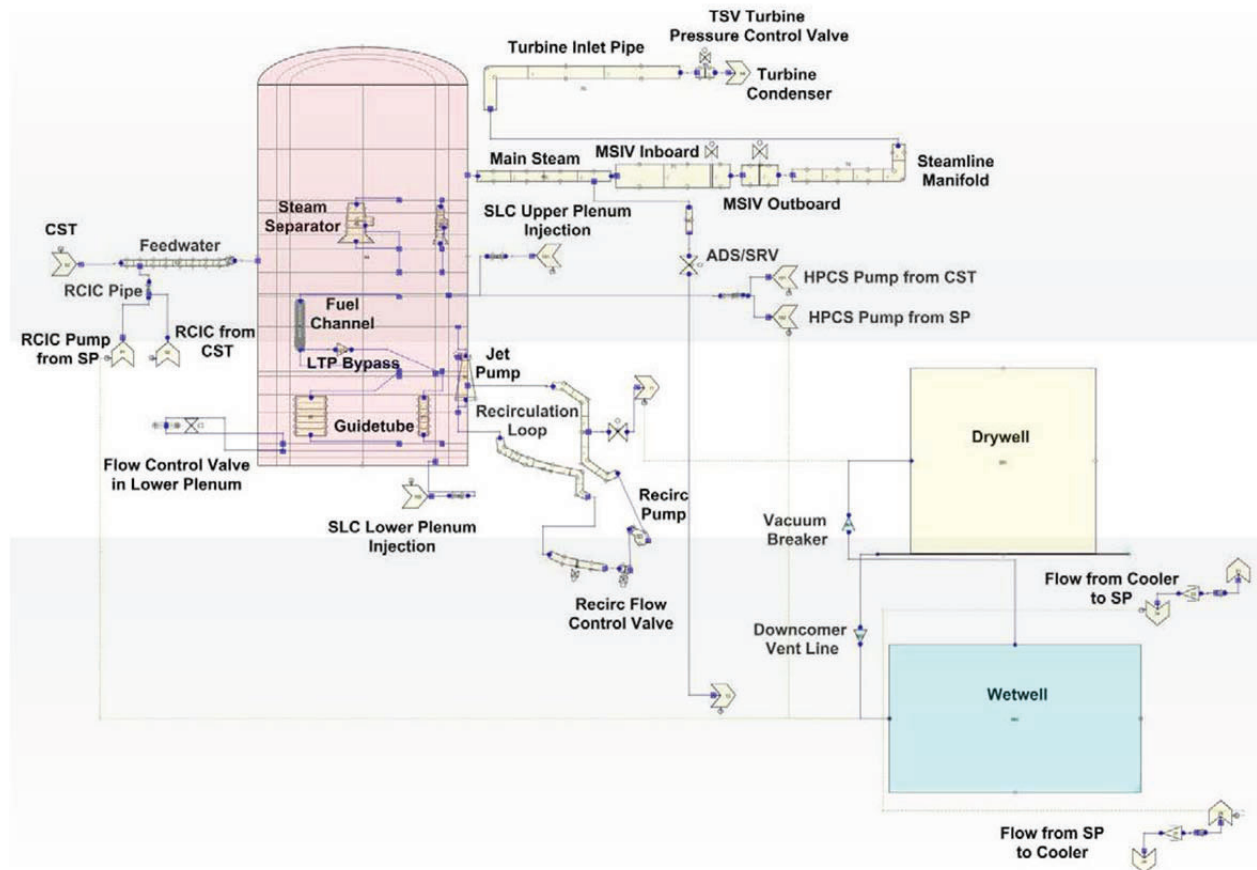


Figure 2. Component View of the BWR/5 Plant for ATWS Simulations [5].

2.2. PARCS Core Model

The models assume an equilibrium core of 764 GE14 assemblies. Fuel enrichment varies from rod to rod, and gadolinia concentration changes for different rod types and axial level. The active core region is modeled with 25 uniform axial nodes. The models include multiple planar regions with unique materials, representing two reflectors (top and bottom), and several distinct axial segments in the active fuel region.

The cross-sections used by PARCS were generated with SCALE/TRITON [9]. The cross section files for the homogenized fuel assemblies include four void histories, multiple burnup steps (up to a maximum exposure of 60 GWd/MTU), and a selection of branches combining five moderator densities, three fuel temperatures, four boron concentrations, and two control states (controlled/uncontrolled).

3. CALCULATION RESULTS AND ANALYSIS

A turbine trip with full bypass (TTWBP) was considered as the ATWS event in the current analysis. The event was considered based on its previous consideration in [10]. Section 3.1 provides an overview of this event. Three initial conditions were considered: beginning of cycle (BOC), peak hot excess (PHE), and end of full power life (EOFPL). For the BOC and PHE cases, the initial core flow rate is 85 percent of the rated core flow (RCF) (corresponding to the low-flow corner of the MELLLA+ domain upper boundary). The EOFPL case is analyzed at a higher flow rate (105 percent RCF) consistent with expected flow conditions near the end of cycle.

Table I. Sequence of Events for TTWBP ATWS-I Event

Time (s)	Event
0.0	<ul style="list-style-type: none"> Null transient simulation starts.
10.0	<ul style="list-style-type: none"> Null transient simulation ends. Turbine trip is initiated by closing the TCV. Recirculation pumps are tripped on the turbine trip. Feedwater temperature starts decreasing.
10.1	<ul style="list-style-type: none"> TCV closes completely and starts opening again to simulate 100 percent turbine bypass flow.
11.1	<ul style="list-style-type: none"> TCV (bypass) completes opening and its open area provides the predetermined steam flow fraction of 100%.
~11.4	<ul style="list-style-type: none"> Steam flow starts decreasing.
~13.0	<ul style="list-style-type: none"> Feedwater flow starts decreasing.
~95	<ul style="list-style-type: none"> Power oscillation above noise level apparent (instability onset) in PHE and BOC No power oscillation in EOFPL.
120	<ul style="list-style-type: none"> Water level reduction is initiated by reducing the normal water level control system setpoint linearly to TAF over 180 s.
130	<ul style="list-style-type: none"> Boron injection is initiated and linearly ramped to full flow at 190 s.
~164	<ul style="list-style-type: none"> Noticeable bi-modal oscillation of the core power is initiated in PHE. ~143 s in BOC. No bi-modal oscillation of the core power in EOFPL.
~160	<ul style="list-style-type: none"> Boron starts accumulating in the core.
~163	<ul style="list-style-type: none"> Downcomer water level begins decreasing in PHE. ~158 s in BOC. ~147 in EOFPL.
~163	<ul style="list-style-type: none"> Peak cladding temperature of ~1,691 K occurs in PHE. ~1,373 K at 181 s in BOC. No significant increase of cladding temperature in EOFPL.
~240	<ul style="list-style-type: none"> Power oscillation ends in PHE. ~245 s in BOC. No power oscillation in EOFPL.
400	<ul style="list-style-type: none"> Simulation ends.

3.1. ATWS-I Event Description

A turbine trip results in closure of the turbine stop valve (TSV), but the expected reactor trip is assumed to fail. The turbine trip signal also initiates a 2RPT. The TSV closure is simulated by rapidly closing the TCV in the TRACE model. Turbine bypass is simulated by reopening the TCV to its initial 100 percent flow area. The 2RPT ramps down the forced recirculation flow as the pumps coast down, and a natural circulation flow develops in the vessel. Isolating the turbine causes a steady decrease in FW temperature because the extraction steam feed to the FW heater (FWH) cascade has been stopped.

The event is mitigated by manual operator actions to lower RWL and inject soluble boron through the SLCS. Table I provides the sequence for the event initiated from the PHE initial condition, but notes any differences for the BOC and EOFPL cases.

3.2. Steamline Flow Rate

Figure 3 shows the steamline flow for all three cases. The steamline flow indicates a sudden decrease at 10 seconds when the TCV closes. There is an accompanying increase in RPV pressure (see Section 3.4 and Figure 6). As the TCV reopens, the steamline flow increases above nominal levels as the dome pressure is higher than the initial pressure. The steamline flow then decreases along with reactor power (see Section 3.3 and Figure 4). Between approximately 100 and 175 s the steamline flow is oscillatory in the BOC and PHE cases, this can be attributed to the power oscillations during the same period. As reactor power decreases long term, the steamline flow rate also decreases. The relatively small steamline flow in the EOFPL case is due to lower core power (see Section 3.3 and Figure 4) than the other two cases.

3.3. Core Power

In response to the TCV closure, the RPV dome pressure increases and voids collapse in the core. This can be seen in the pressure response (Section 3.4) and RWL response (Section 3.7). In response to the void collapse the reactor power increases sharply, see Figure 4. The reactor power increase is terminated by a combination of effects. One is the Doppler effect which adds negative reactivity in response to increasing fuel temperature. The second is the effect of the 2RPT on core flow (Section 3.5). Following the turbine trip, an automatic 2RPT reduces core flow. The effect of the reduced core flow, combined with increased heat flux following the initial increase in reactor power, leads to prompt void production in the core and the addition of negative void reactivity to the core. As natural circulation conditions develop in the system, the reactivity feedback stabilizes the reactor power at a condition that maintains a critical void fraction distribution in the reactor core.

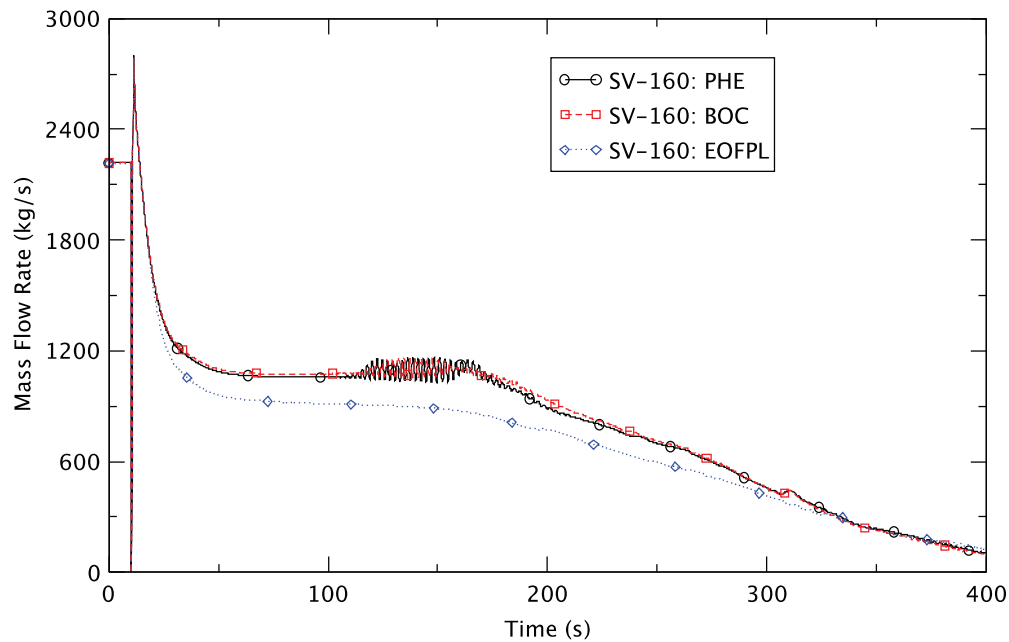


Figure 3. Steamline Flow Rate.

Following the decline in power from ~11 to 25 s, the reactor power begins to increase. This increase in reactor power is due to an increase in inlet subcooling (Section 3.6). While reactor power is increasing, the steamline flow is relatively stable. This is because the increased reactor power is compensating for the increased subcooling.

The EOFPL case power is lower in the natural circulation phase compared to the BOC and PHE cases. This is attributed to the higher initial core flow for the EOFPL case (105 percent RCF compared to 85 RCF) and its correspondingly lower core average void fraction. After the 2RPT the reactor stabilizes at a new state under natural circulation. At this new, quasi-critical state, the core average void fraction remains quite similar (accounting for other, secondary reactivity feedback mechanisms) to the core average void fraction before the 2RPT. A lower initial core average void fraction for the EOFPL case leads to a lower core average void fraction, under natural circulation, than the other two cases. Under natural circulation the core average void fraction varies with power (see Section 3.5). The lower critical average void fraction in the EOFPL case, along with a similar core flow rate to the BOC and PHE cases (see Figure 7), results in a lower power after the 2RPT.

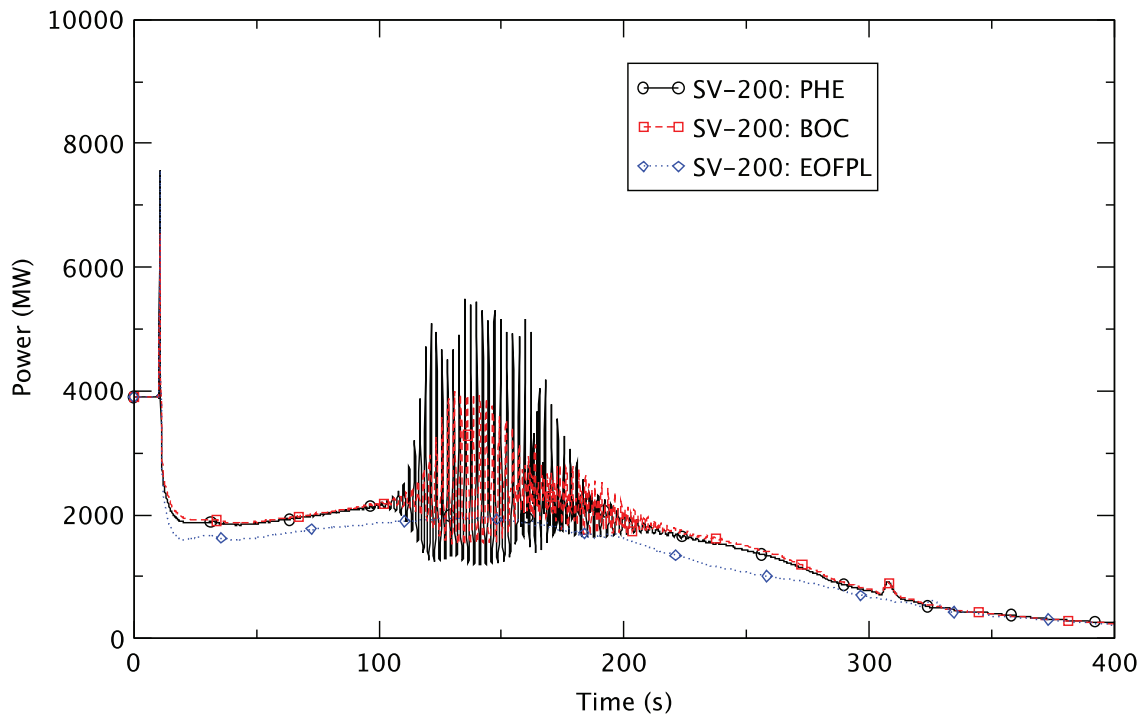


Figure 4. Reactor Power

As the subcooling increases in the first 100 s, the boiling boundary begins to penetrate deeper into the core and the reactor power axial distribution shifts towards the bottom of the core. The bottom peaked power shape combined with high power and low flow conditions leads to an unstable configuration. At approximately 95 s, growing power oscillations are observed in the PHE and BOC cases. No such power oscillations are observed in the EOFPL case. This lack of power oscillation in the EOFPL case is primarily attributable to two factors. First, the EOFPL case initiates from a higher initial core flow rate, as such, the gross reactor power following 2RPT is lower while the core flow rate is largely the same when compared to the other cases (see Figure 7). Additionally, the EOFPL axial power distribution is top-peaked. The combination of these two factors makes the core in the EOFPL case more stable.

The power oscillations in the PHE case reach a large amplitude, larger than in the BOC case. In addition, around 150 seconds, the PHE power response shows what appears to be a doubling of the oscillation frequency. This frequency doubling is a tell-tale indication of non-linear bi-modal coupling. This is a phenomenon where the core-wide and out-of-phase harmonic modes are both sufficiently unstable that second order coupling results in the evolution of a bi-modal oscillatory behavior. Figure 5 illustrates the onset of the bi-modal oscillation. In these figures each box represents a fuel bundle in the reactor core, and the height of each box corresponds to the power of that bundle.

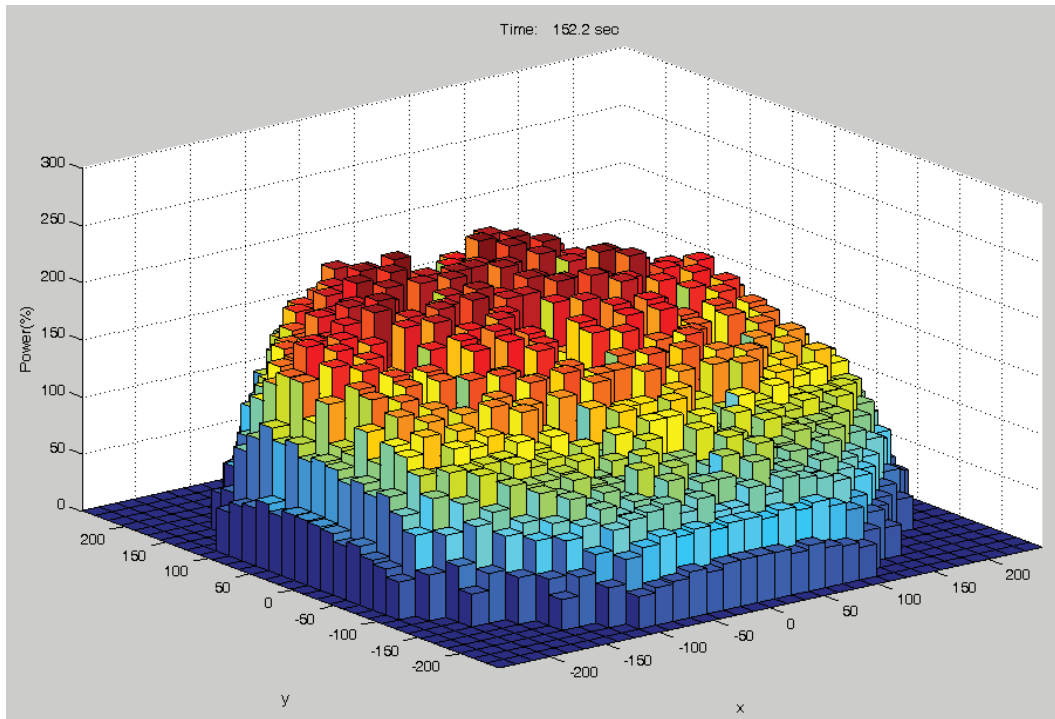


Figure 5. Recognizable Bi-modal Oscillation of Power at 152.2 s in PHE Case

After 150 seconds the reactor power oscillation amplitude and average reactor power can be seen decreasing in Figure 4. This can be attributed to manual operator actions reduce RWL and inject soluble boron. As discussed in Section 3.6, the reduced water level reduces inlet subcooling, which in turn reduces reactor power. Further, the introduction of soluble boron at 130 s is “felt” by the reactor core around 20-30 s later (see Section 3.8). The combination of these actions can be seen to be effective in suppressing the power oscillation and reducing total core power.

3.4. RPV Dome Pressure

Figure 6 provides a plot of the transient RPV dome pressure for all three cases. The responses are relatively similar to each other. The pressure initially spikes in responses to the turbine trip. After the TCV reopens, the effect of the turbine bypass is to reduce and control dome pressure. Because of the operation of the TBS, the SRVs are not predicted to lift in any of the simulation cases.

3.5. Core Flow

Figure 7 shows the core flow response. The initial core flow rate for the BOC and PHE cases is 85 percent of RCF while it is 105 percent RCF in the EOFPL case. Following the 2RPT, all three cases illustrate the decline of core flow during the pump coastdown and the evolution of a natural circulation flow rate.

The core flow rate is very similar among all three cases following 2RPT. This is because under conditions of natural circulation, the core pressure drop is relatively insensitive to reactor power. For higher power conditions (i.e. PHE and BOC) the higher void production in the core tends to reduce core average coolant density and the associated gravitational pressure drop, but also to increase pressure drop

due to two phase friction effects. These two effects seem to be offset by each other and the pressure drop remains similar. Since core pressure drop becomes essentially independent of the power in these cases, the flow rate is largely determined by the RWL response (Section 3.7 and Figure 10). Since the level is controlled by the same control system in all three cases, the level response is very similar. The end result being that all three cases show essentially the same core flow response.

3.6. Core Inlet Subcooling

The instability onset in the PHE and BOC cases around 95 seconds is due to increased inlet subcooling. Figure 8 provides a plot of the subcooling response. The subcooling initially increases because the feedwater entering the reactor vessel becomes colder. When the turbine trips, extraction steam is isolated from the FWH cascade. In response, FW temperature slowly decreases (taking into account for the thermal inertia of the FWH cascade). As FW temperature decreases, but level is maintained, the net effect is an increase in core inlet subcooling.

The inlet subcooling response for the EOFPL case is milder compared to the PHE and BOC cases. This is because reactor power (and hence steam production rate) is lower in the EOFPL case. The lower steamline flow rate means that the FW flow rate is also lower for the EOFPL case (see Section 3.7 and Figure 9). A lower FW flow compared to the other case means a reduced response to the lower FW temperature compared to the other two cases.

When operators begin to control RWL to a lower level, the FW flow is reduced around 130 s (Section 3.7). This reduction in FW flow reduces the injection of cooler water into the downcomer and results in a reduction of the core inlet subcooling.

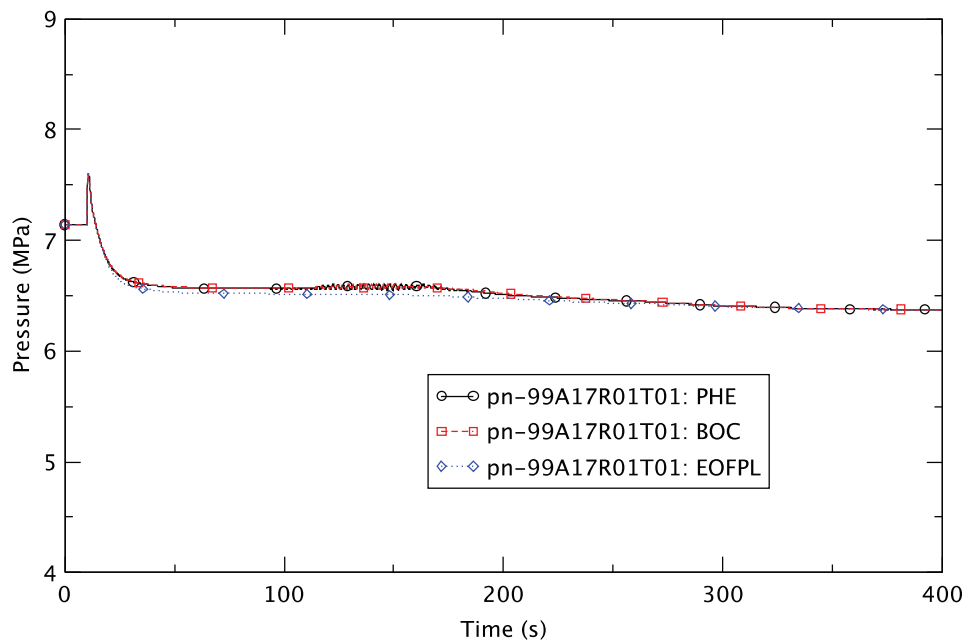


Figure 6. Dome Pressure.

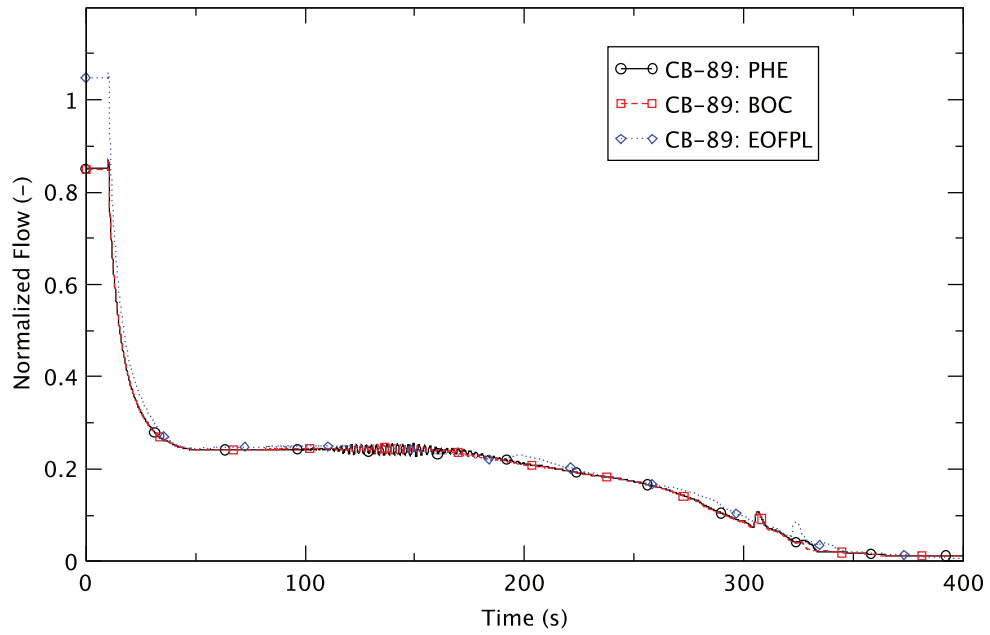


Figure 7. Normalized Core Flow.

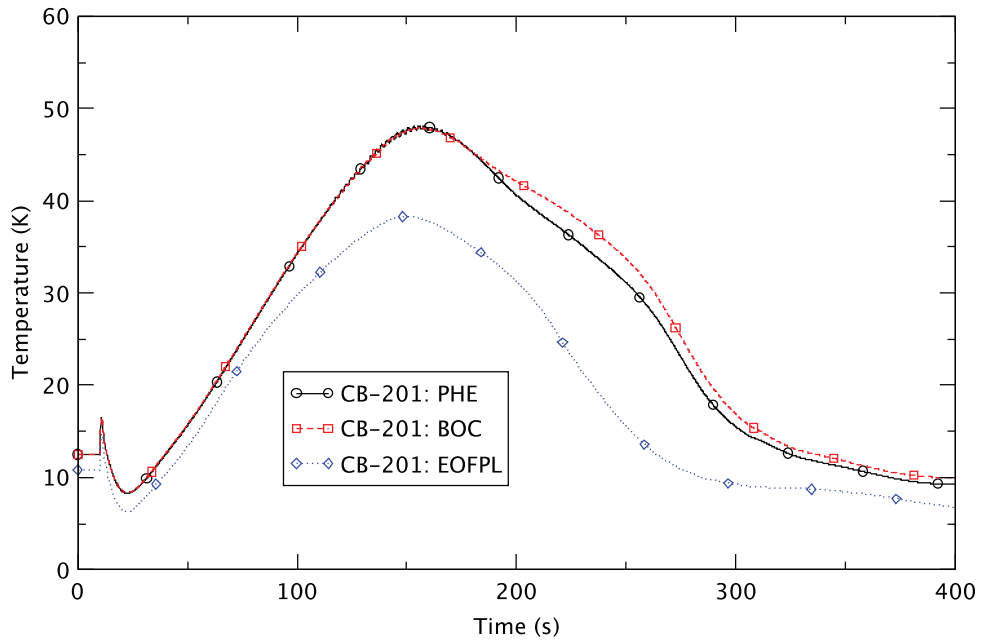


Figure 8. Inlet Subcooling.

3.7. Feedwater Flow and RPV Water Level

Figure 9 provides the response of the FW flow and Figure 10 provides the RWL response. The Initial FW flow response shows a sharp decrease, and this is due to the nature of the three-element controller responding to the sudden decrease in steam flow rate when the TCV closes. The FW flow recovers when the valve reopens to simulate the TBS. The EOFPL FW flow rate from ~25 to 270 s is lower compared to the BOC and PHE cases. This is caused by the lower power, and hence lower steam flow rate in the EOFPL case. The amount of FW to maintain the same level at a lower reactor power is lower.

The FW response indicates a more dramatic decline following 130 s. This is in response to the simulation of the manual operator actions to control water level to TAF. Figure 10 illustrates the effect of this simulated manual operator action as level can be seen to decrease and then eventually level out around 350 s. The intention of lower reactor water level is twofold. First, the lower RWL will lower core flow rate and hence reactor power, second lowering the RWL will uncover the FW spargers. Uncovering the spargers allows the injected FW flow to condense steam in the downcomer region before entering the jet pump. The increased subcooling is due to the lower FW temperature, but if level drops below the sparger, condensation heat transfer in the downcomer can be effective in erasing the inlet coolant subcooling.

Around 150 s the subcooling trend reverses (see Figure 8). This initial turn around in the response is not due to condensation heat transfer, but rather just in response to a reduced flow rate of cold injection from the FW system.

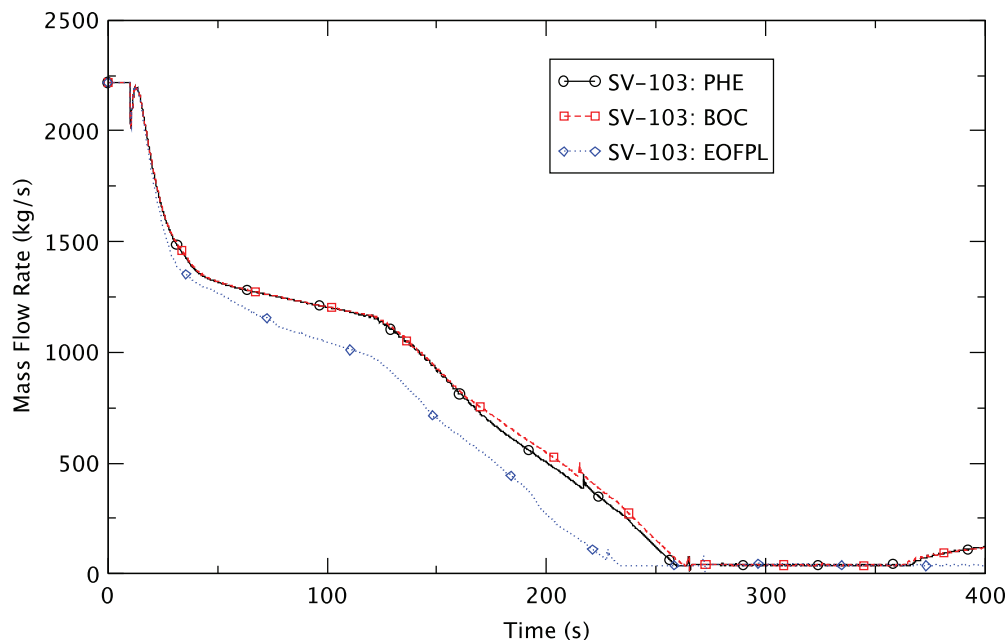


Figure 9. Feedwater Flow.

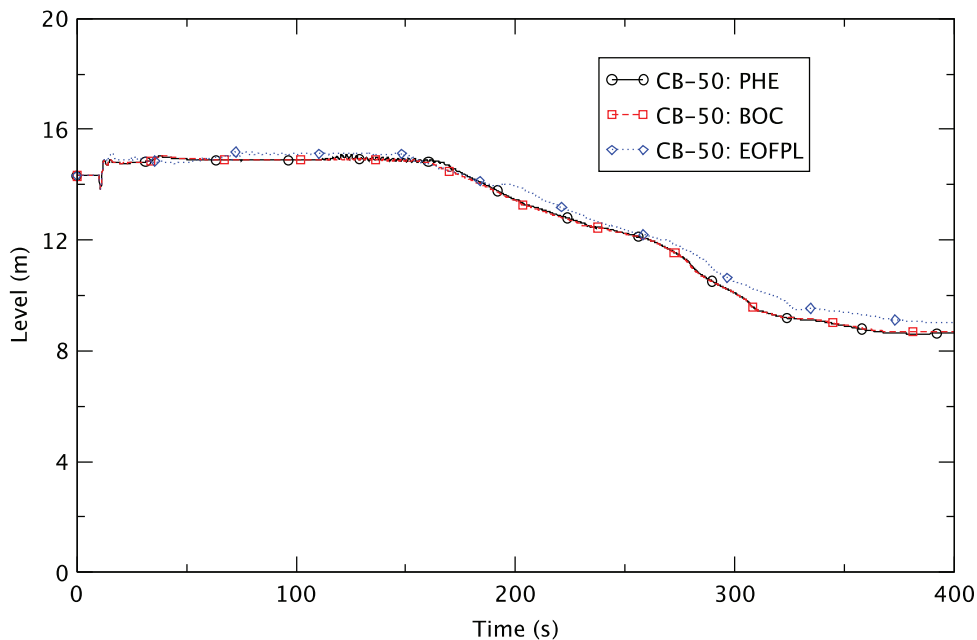


Figure 10. Downcomer Water Level.

3.8. Boron Inventory in the Core

Figure 11 illustrates the core inventory of soluble boron. The core inventory begins to increase in all cases around 150 s. The incursion of boron to the core slightly lags the introduction of boron to the vessel via the SLCS because the injection point is into the upper plenum. Under ATWS conditions, the steam flow rate in the upper plenum is sufficient to entrain the injected SLCS flow. The borated liquid then flows to the downcomer from the separators and circulates to the core through the lower plenum. This results in a delay of 20-30 s, corresponding to the transit time from the upper plenum to core inlet.

The boron accumulation rates are essentially identical as the rate of delivery is driven almost exclusively by the core flow rate, which is essentially the same in all three cases, as discussed in Section 3.5.

3.9. Fuel Cladding Temperature

Figure 12 illustrates the core-wide peak cladding temperature (PCT) for all three cases. The EOFPL case does not indicate any degree of fuel heat-up. This is because this case does not evolve to unstable power oscillations. In the BOC and PHE cases, the fuel temperature increases during the large amplitude power/flow oscillation stage of the event. As can be seen, there are phases in both cases of periodic cladding dryout and rewet. In the BOC case this period is relatively long and occurs between about 120 and 140 s. A corresponding trend is also seen in the PHE case between about 120 and 125 s.

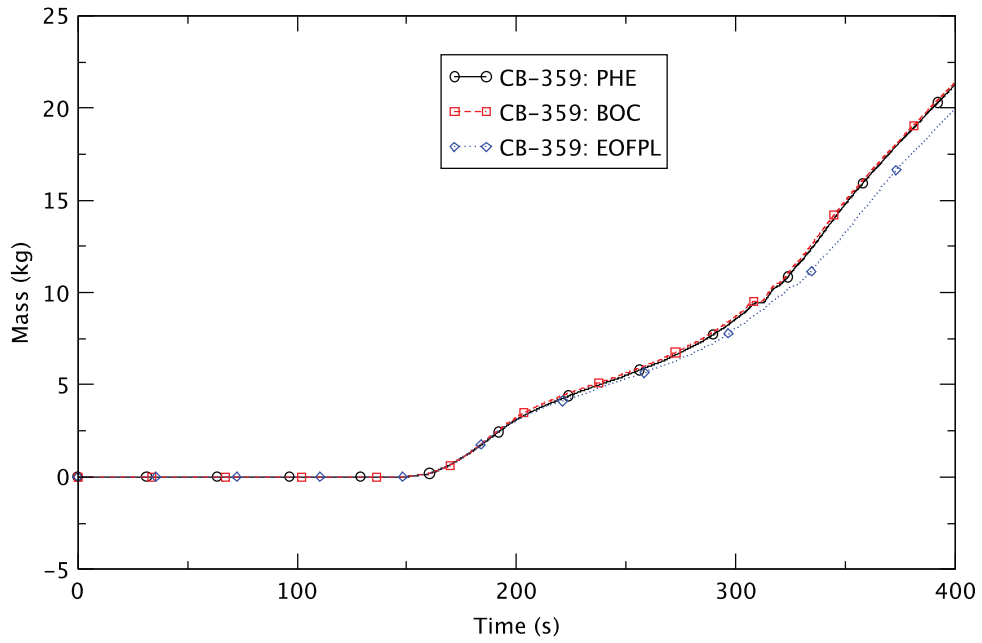


Figure 11. Core Boron Inventory.

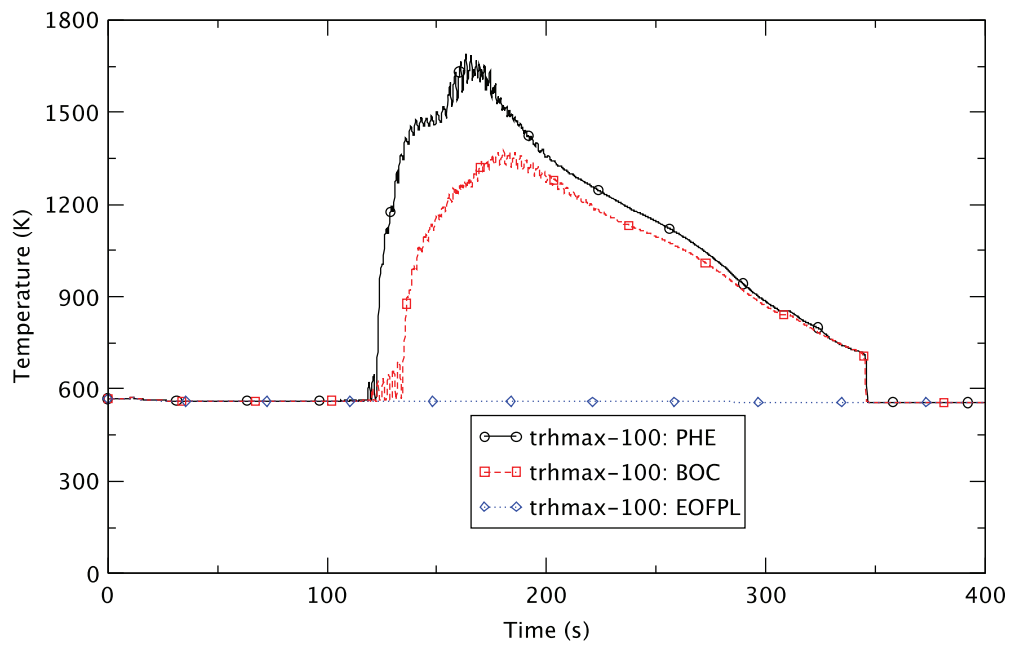


Figure 12. Peak Cladding Temperature.

The sudden increase in cladding temperature following the cycles of dryout/rewet occurs when the fuel temperature exceeds the minimum stable film boiling temperature (T_{min}). In the region of the hot spot, the channel flow oscillations are severe, in some cases and times resulting in substantial flow reversal. During the low flow stage of the oscillation the cladding surface is predicted to enter post-critical heat flux (CHF) dryout. This duration is relatively short as the oscillation frequency is about 0.4 Hz. However, during that post-CHF dryout period, the cladding temperature increases. During the positive flow part of the oscillation, the cladding surface is able to rewet and heat is removed.

In the PHE and BOC cases, however, not all of the energy deposited in the fuel during the post-CHF dryout phase is fully removed during the rewet phase of the oscillation. The cladding surface temperature then begins to “ratchet” up. This can be seen by the increasing height of the successive PCT peaks in the dryout/rewet period as shown in Figure 12. When the cladding surface temperature reaches T_{min} the heat transfer regime is then “locked” into a film boiling regime, which has a low heat transfer coefficient. This regime persists until the cladding surface temperature is brought below T_{min} and the surface can rewet. In the current calculations, the void fraction oscillates in the hot spot vicinity as well, ranging between ~5 and ~95 percent. As such the regime also oscillates between inverted annular film boiling at times of low void fraction where a vapor blanket around the cladding hot spot is predicted and dispersed flow film boiling at times of high void fraction.

The calculation results here demonstrate a possible mechanism whereby the fuel may become damaged. During large amplitude power/flow oscillations, a phase of periodic dryout/rewet may occur. If the oscillations in flow are of a sufficient magnitude, the heat deposited in the fuel during the dryout phase cannot be totally removed during the rewet phase. When this occurs the cladding surface temperature will ratchet up. If the oscillations then persist, the cladding surface temperature will reach T_{min} and the surface will become locked into the film boiling heat transfer regime. Once this lock occurs, the cladding temperature will increase dramatically until the reactor power can be reduced using emergency operating procedure actions.

4. CONCLUSIONS

This study analyzed the BWR/5 response to an ATWS initiated by a turbine trip while operating at MELLLA+ conditions. Three ATWS-I cases were considered using the coupled code system TRACE/PARCS to investigate the effectiveness manual operator actions on reactor instability and the ability to cope with the failure of a reactor trip. The findings from the simulation were examined carefully and our conclusions from the analysis are summarized below.

1. The most severe reactor instability is predicted at PHE. This is based on using the peak clad temperature as the metric for the margin to safety for an ATWS event.
2. TRACE predicts that the operator’s manual actions recommended by the emergency procedure guidelines (namely reducing water level and injecting boron) are effective in suppressing unstable power oscillations that develop during the ATWS-I event. The action to reduce level is effective insofar as lowering the FW flow contributes to limiting the increase in core inlet subcooling.
3. TRACE predicts that the PCT exceeds the fuel damage threshold of 1,478 K [2,200°F] in the limiting case at PHE. The PCT excursion is due to a failure to rewet once local power oscillations have resulted in the temperature of the cladding exceeding T_{min} .
4. In all cases, the effect of the operator’s action of level reduction to the TAF at 120 s is delayed by 20 s. The onset of core power oscillations occurs earlier than the time of the decrease in downcomer water level in all cases. The onset of decay of the power oscillations, in terms of the highest local power peaking factor, takes place in all cases after the DC level has dropped and boron has built up in the core.

5. TRACE calculates a 20-30 s delay for the boron to reach the core after injection into the RPV that starts at 130 s. Boron contributes to suppressing power oscillations in the reactor, and maintains the core in cold shutdown over the long term.
6. The time in a fuel cycle has an impact on reactor instability. The most unstable reactor condition is predicted at PHE and intermediate reactor instability at BOC, even though the general behavior of the important parameters affecting reactor instability is very similar for both cases. The reactor does not develop any significant power oscillations at EOFPL. The relative stability therein is attributed to a combination of factors: a relatively lower core power after the 2RPT, a lower liquid subcooling at the core inlet, and an axially top-peaked core power shape.
7. The current assumption of half-core symmetry in the mapping of hydraulic channels may be inadequate to resolve higher harmonic modes in the core response. This is particularly true for regional oscillations where the axis of symmetry may rotate in the core.

ACKNOWLEDGMENTS

The authors would like to acknowledge Matthew Jesse and Brian Ade from Oak Ridge National Laboratory and Scott Krepel of the NRC staff for their contributions in the area of cross-section generation, Harold Scott of the NRC staff for performing the FRAPCON calculations, Matthew Bernard of the NRC staff for TRACE code support, Stephen Bajorek and Joseph Staudenmeier of the NRC staff for their contributions to the analysis, and Istvan Frankl and Tarek Zaki of the NRC staff for serving as project managers.

REFERENCES

1. "TRACE V5.0 Theory Manual," U.S. Nuclear Regulatory Commission, June 4, 2010 (ADAMS Accession No. ML120060218).
2. T. Downar, et al., "PARCS: Purdue Advanced Reactor Core Simulator," *Proceedings of Reactor Physics Topical Meeting (PHYSOR 2002)*, Seoul, Korea, October 7-10, 2002 (2002).
3. J. Harrison, GE Hitachi, letter to U.S. Nuclear Regulatory Commission, "Accepted Version of GE Licensing Topical Report NEDC-33006P-A, Revision 3 (TAC No. MD0277)," MFN 09-362, June 19, 2009, (ADAMS Accession No. ML091800512).
4. P. Yarsky, "Applicability of TRACE/PARCS to MELLLA+ BWR ATWS Analyses, Revision 1," U.S. Nuclear Regulatory Commission, Office of Nuclear Regulatory Research, November 18, 2012, ADAMS Accession No. ML113350073.
5. L. Cheng, et al., "TRACE Model for Simulation of Anticipated Transients Without Scram in a BWR," *Trans. Am. Nucl. Soc.*, Washington, DC, November 10-14, 2013, Vol. 109, pp. 987-990 (2013).
6. L. Cheng, et al., "TRACE/PARCS Core Modeling of a BWR/5 for Accident Analysis of ATWS Events," *Trans. Am. Nucl. Soc.*, Washington, DC, November 10-14, 2013, Vol. 109, pp. 979-982 (2013).
7. P. Yarsky, "TRACE/PARCS Evaluation of Potentially Limiting ATWS Events with Core Instability for the ABWR," *Proceedings of International Congress on Advances in Nuclear Power Plants (ICAPP) 2013*, Jeju Island, Korea, April 14-18, 2013 (2013).
8. A. Wysocki, et al., "TRACE/PARCS Analysis of Out-of-Phase Power Oscillations with a Rotating Line of Symmetry," *Proceedings of 15th International Topical Meeting on Nuclear Reactor Thermal-Hydraulics, NURETH-15*, Pisa, Italy, May 12-17, 2013 (2013).
9. Oak Ridge National Laboratory, SCALE: A Comprehensive Modeling and Simulation Suite for Nuclear Safety Analysis and Design, ORNL/TM-2005/39 (2011).
10. NEDO-32047-A, "ATWS Rule Issues Relative to BWR Core Thermal-Hydraulic Stability," June 1995